# Dalton Transactions

Accepted Manuscript






ROYAL SOCIETY OF CHEMISTRY

www.rsc.org/dalton

Journal Name

RSCPublishing

ARTICLE

# Homopolar dihydrogen bonding in main group hydrides: discovery, consequences, and applications

Cite this: DOI: 10.1039/xoxxooooox

David J. Wolstenholme,* Jessica L. Dobson and G. Sean McGrady*

Received ooth January 2012,
Accepted ooth January 2012

DOI: 10.1039/xoxxooooox

www.rsc.org/

This perspective describes the recent discovery and investigation of homopolar dihydrogen bonding, and focuses on the identification and characterisation of hydride-hydride interactions in compounds of the main group elements. A highlight of this program has been an appreciation of the important role played by this interaction in the structural and thermochemical properties of these materials, and in the mechanisms through which they release hydrogen. A fuller understanding of this new class of H···H interactions has also allowed us to explore their role in the supramolecular chemistry of hydrogen-rich compounds.

## 1. Introduction

The unique nature of hydrogen, with its non-directional valence orbital and lack of any core electron density, allows this atom to engage in a multitude of diverse interactions (Scheme 1), many of which were counter-intuitive prior to their discovery. The concept of hydrogen bonding was initially proposed in 1912 by Moore and Winmill, to account for the change in basicity on going from trimethylammonium hydroxide to its tetramethylammonium derivative.[1] These fundamental interactions have since been shown to play a central role in many chemical, physical, and biochemical processes.[2-4] The unique and chemically unparalleled nature of hydrogen bonding led Pauling to describe the phenomenon as thus: "*under certain conditions an atom of hydrogen is attracted by rather strong forces to two atoms, instead of one, so that it may be considered to be acting as a bond between them*".[5] Furthermore, he pointed out that the hydrogen atom is generally situated between the most electronegative atoms. This is exemplified by the bifluoride ion, $[FHF]^-$, in which a proton interacts symmetrically with two fluoride ions.[6] Pauling's definition of hydrogen bonding was consistent with an earlier model proposed by Lewis, who stated: "*an atom of hydrogen may at times be attached to two electron pairs of two different atoms*".[7]

In 1960, Pimentel and McClellan recognised that the rapidly growing body of work concerning hydrogen bonding was not exclusive to strong symmetric interactions, but rather that there exists a broad range of X-H···Y interactions of varying strength and geometry.[8] This realisation prompted them to survey the phenomenon, and to propose a more convenient definition of hydrogen bonding: "*a hydrogen bond exists between a functional group A-H and an atom or group of atoms B in the same or a different molecule when there is evidence of bond formation (association or chelation) and there is evidence that this new bond linking A-H and B specifically involves the hydrogen atom already bonded to A*".[8] This expanded view of hydrogen bonding provided an opportunity for researchers to extend the concept to include unconventional interactions, and to lay the foundations for the emergence of the field of supramolecular chemistry. For example, short C-H···O contacts would not be considered hydrogen bonds under Pauling's definition, since a C-H moiety does not contain an electronegative atom. Nevertheless, these interactions are now widely accepted as weak hydrogen bonds, and they play a pivotal role in stabilising the extended structures of countless systems.[9] Thus, conventional hydrogen bonding can be more usefully summarised as a positively charged hydrogen donor interacting with an appropriate Lewis base acceptor.

More recently, the concept of hydrogen bonding has been extended to include proton–hydride interactions, in which a hydridic moiety, rather than a non-bonding electron pair, serves as the acceptor in an X-H···H-Y interaction.[10] This type of interaction was first recognised by Brown et al. in the late 1960s, who showed that Lewis acid-base adducts containing an $L{\cdot}BH_3$ (L = $Me_3N$, $Et_3N$, etc…) moiety engaged in weak H···H interactions in the presence of a proton donor (MeOH).[11] A subsequent survey of the Cambridge Structural Database (CSD) for short H···H contacts in N-B complexes (1.7-2.2 Å) revealed a distinct preference for a bent geometry for these interactions, in contrast to the more linear disposition of their X-H···Y counterparts.[12] This showed that the NH···H-B angles generally fall between 95 and 120°, whereas the N-H···HB angles are closer to linear (150-170°). Such a geometry is consistent with the hydridic nature of the B-H moiety, as the bent configuration allows the approach of the N-H group to maximise the electrostatic component of the interaction. Furthermore, a series

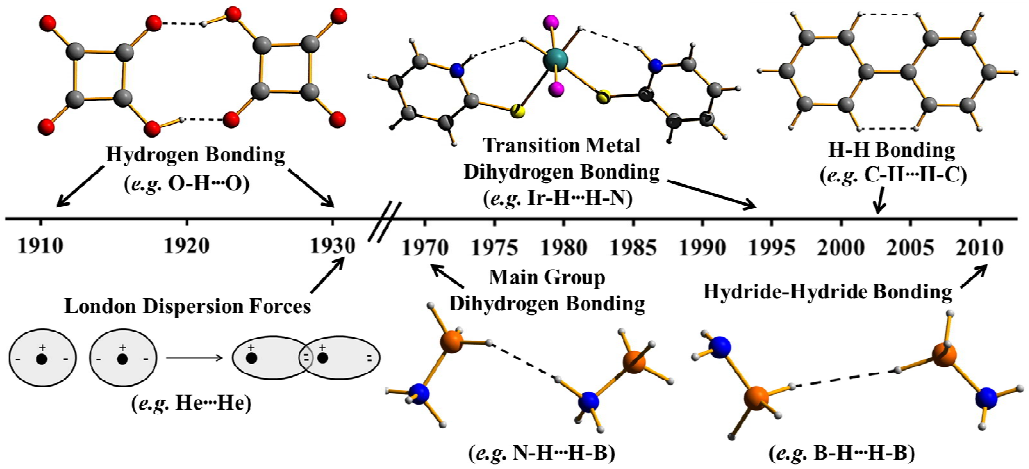


**Scheme 1.** Historical perspective on the progression of hydrogen bonding and related interactions.

of calculations involving the interaction of metal hydrides with HF revealed that the strength of these dihydrogen bonds is highly correlated with their H···H distances, consonant with the behaviour of X-H···Y hydrogen bonds.[13,14]

In 1994, Crabtree and Morris each independently discovered the existence of proton-hydride interactions in transition metal hydride complexes.[15,16] Crabtree et al. found that an iridium hydride amide complex tautomerised to the iminol form on account of a stabilising Ir-H···H-O interaction.[15] However, the H···H distance in this structure could not be determined, owing to the uncertainty in the position of the hydride moiety. Accordingly, $^1$H NMR $T_1$ relaxation measurements in solution were used to estimate the H···H distance (~1.8 Å). It is noteworthy that this value falls in the shorter regime identified by the earlier CSD survey and corresponds to a moderately strong interaction, as reflected by large coupling constant between the Ir-H and O-H moieties.[12,15] These conclusions are also consistent with the short H···H contacts (~1.75 Å) determined by Morris et al. through $^1$H NMR $T_1$ relaxation measurements in solution for a similar Ir-H complex.[16] Hoffman and co-workers explored this novel form of hydrogen bonding using a slightly modified version of the structure reported by Morris et al., with the calculations (RHF/6-31G*) showing that the attractive H···H interactions are primarily electrostatic in nature.[17] These pioneering studies laid a sound foundation for our understanding of dihydrogen bonding in both main group and transition metal compounds, and the phenomenon is now widely exploited in areas as diverse as supramocular chemistry and organometallic catalysis.[18-20]

The ability of proton-hydride bonding to influence the structure and reactivity of hydrogen-rich materials is intuitive, since the strong electrostatic attraction between the oppositely charged hydrogen atoms will encourage the formation of an interaction.[10-20] In contrast, it is quite counter-intuitive to consider an attractive scenario for close homopolar dihydrogen contacts. Nevertheless, non-polar C–H moieties have recently been shown to engage in mutually stabilising C-H···H-C interactions.[21,22] The partial charges associated with the hydrogen atoms of the C-H moieties are often small but not necessarily of opposite signs, suggesting that homopolar dihydrogen bonding is not dominated by electrostatics, but rather is underpinned by a substantial contribution from van der Waals attraction.[23] These H···H interactions can therefore be usefully compared to classical examples of London dispersion forces, in which an induced dipole moment results in two fluctuating electron densities that interact to stabilise the corresponding molecular aggregate.[24]

The identification and characterisation of homopolar dihydrogen bonding (*i.e.* C-H···H-C) in both the gas-phase and solid-state structures of organic compounds prompts the following questions: can two hydridic hydrogen atoms engage in a similar interaction in metal or molecular hydrides? If so, can this interaction contribute to the structural and chemical nature of these hydrides? This perspective article attempts to answer these questions in the light of our recent work on the structure-bonding-reactivity relationship for hydride materials of the main group elements. This program was initiated following our discovery of a novel class of homopolar dihydrogen bonding, which we have termed hydride-hydride interactions, both to place them in context with but also to distinguish them from more conventional proton-hydride bonding. In the following sections we describe the discovery and characterisation of these remarkable H···H interactions, and we discuss their consequences and applications.

## 2. Atoms in Molecules (AIM)

A full characterisation of hydrogen bonding and related interactions has traditionally relied on the availability of accurate geometrical parameters from solid-state structures. However, significant advances in computational techniques and theory over the past few decades have allowed researchers to explore the boundaries in our understanding of chemical bonding. Over this period the quantum theory of "*Atoms in Molecules*" (AIM) has emerged as an attractive and powerful method for interpreting subtle chemical details of a material based on its electron distribution.[25] This approach has seen tremendous success in analysing a wide range of weak interactions for both gas-phase and solid-state systems.



 

Accordingly, our analysis of homopolar dihydrogen bonding has largely relied on AIM theory, and we present here a brief introduction of its main concepts. The reader is directed to several excellent reviews for a more detailed description of this method.[26]

The AIM methodology is based primarily on a partitioning of space using the gradient of the electron density, $\nabla\rho(r)$.[25] When the null vector differs from the gradient and an equation of a surface is of the form $\rho(r)$ = constant, then the $\nabla\rho(r)$ evaluated at any particular point in space will be normal to the surface at that location.[25] A series of these points are referred to as a gradient path, and they represent the curve in which its vector is tangential at each point. This theory states that all gradient paths will coalesce at points where $\nabla\rho(r)$ is zero, which corresponds to a maximum, minimum, or saddle point in the electron density.[25] These special points in space are denoted as critical points (CPs), and are classified by calculating and diagonalising the Hessian matrix of the electron density, $\nabla\nabla\rho(r)$. This mathematical manipulation leads to three non-zero eigenvalues (curvature of the gradient), three eigenvectors (direction of the curvature), and the corresponding signs of these eigenvalues. These CPs can then be sub-divided into four categories based on the sum of their eigenvalue signs.

- Nuclear Attractor (NCP): all curvatures are negative (3,-3), leading to a local maximum in the density that pertains to the core electrons surrounding a nucleus.
- Bond (BCP): two curvatures are negative and the third is positive (3,-1), indicating that the density increases in one direction and decreases in all others, resulting in a saddle point between two interacting atoms.
- Ring (RCP): two curvatures are positive and the third is negative (3,+1), giving rise to another saddle point in the density that is located within a cyclic arrangement of atoms.
- Cage (CCP): all curvatures are positive (3,+3), emphasising the presence of a minimum in the density. This type of CP is found in the interior of a cluster (or cage) of bonded atoms.

A collection of gradient paths gives rise to a gradient vector field consisting of zero-flux surfaces (2D planes in which the density is a minimum perpendicular to the surface).[25] This topology produces boundaries between neighbouring atoms, allowing for the partitioning of a system into mutually exclusive regions of space known as atomic basins. This concept is central to AIM theory, in which two interacting basins (or atoms) are connected by a maximum line of electron density, commonly referred to as a bond path (BP).[25] The presence of a BP and BCP between two atoms is considered essential for an interaction, with the properties of the BCP often being used to characterise the exact nature of chemical bonding.

The accumulation of electron density at the BCP, $\rho_b(\mathbf{r})$, represents an important parameter for elucidating the behaviour of two interacting atoms. In general, covalent bonds tend to result in large $\rho_b(\mathbf{r})$ values (>0.50 eÅ$^{-3}$), since they involve a considerable sharing of electron density; weaker closed-shell interactions (*i.e.* hydrogen bonding) typically display values ranging from ~0.02 to 0.50 eÅ$^{-3}$.[25,26] This disparity arises because of the strong correlation between the electron density at the BCP and the strength of an interaction. Pioneering studies by Espinosa et al. confirmed this relationship for closed-shell interactions, with the experimental $\rho_b(\mathbf{r})$ values for 83 hydrogen bonds of the form X-H···O (X = C, N, and O) being indirectly related to the dissociation energies of similar calculated interactions.[27] It is notable that such a trend was also observed for both heteropolar and homopolar dihydrogen bonding (N-H···H-B and C-H···H-C).[13,28] The ability to estimate the relative strength of an interaction based on its $\rho_b(\mathbf{r})$ value offers a powerful metric for deconvoluting the stabilising contribution of each type of interaction, and how these influence the packing and orientation of molecules in a crystalline framework.

## 3. Homopolar Dihydrogen Bonding in Binary and Complex Metal Hydrides

Binary and complex metal hydrides are in the vanguard of candidates for hydrogen storage, owing to their high gravimetric and volumetric hydrogen contents.[29] This has prompted a considerable amount of research focused on determining empirically the thermal properties of these systems and their hydrogen release characteristics. In contrast, details of the intimate interactions responsible for initiating and mediating the release of hydrogen have been less well characterised. Thermal decomposition of metal hydrides requires the eventual interaction of two hydridic moieties, in spite of strong electrostatic repulsion imposed on their congress. The following sections describe the prevalence of hydride-hydride interactions in several important binary and complex metal hydrides of interest to the hydrogen storage community, along with a discussion of their role in the evolution of hydrogen.

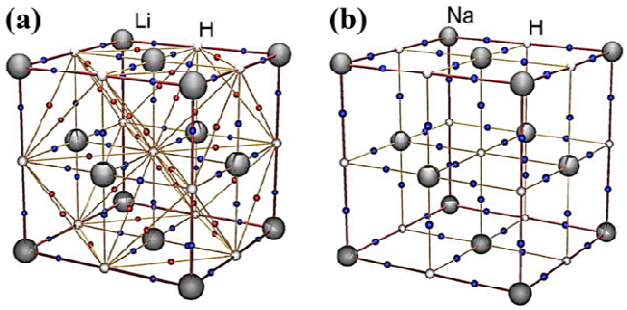


**Figure 1.** Calculated molecular graphs for the unit cells in (a) LiH and (b) NaH. The M-H and H···H BCPs are represented as blue and red dots, respectively. Reprinted from ref. 32 with the permission of Wiley VCH. Copyright 2012 Wiley-VCH.

**3.1 Group 1 Hydrides.** Alkali metal hydrides represent the simplest examples of binary systems capable of liberating hydrogen via homopolar dihydrogen bonding. The structures of LiH and NaH each crystallise in the rock salt lattice *Fm-3m* (#225), with the hydride ions occupying all of the octahedral holes in an fcc array of metal cations.[30] This packing motif gives rise to H···H contacts that exceed the sum of the van der Waals radii for two interacting hydride ions (>2.80 Å).[31] However, our recent topological analysis of LiH, using high-level periodicity calculations in tandem with the

**Table 1.** Topological properties of the electron density for the calculated M-H and H···H interactions in the solid-state structures of select binary and complex metal hydrides (distance in Å, electron density - $\rho_b(\mathbf{r})$ in eÅ$^{-3}$, and hydrogen desorption temperatures - $T_{des}$ in °C).

| Complex | Moiety | Distance | $\rho_b(r)$ | Moiety | Distance | $\rho_b(r)$ | $T_{des}$ | Ref |
|---|---|---|---|---|---|---|---|---|
| LiH | Li-H | 2.014 | 0.101 | H···H | 2.848 | 0.069 | 720 | 32 |
| NaH | Na-H | 2.421 | 0.075 | H···H | 3.423 | - | 425 | 32 |
| $MgH_2$ | Mg-H | 1.945-1.958 | 0.188-0.192 | H···H | 2.507 | 0.132 | 330 | 32 |
| $MgH_2$[†] | Mg-H | 1.935-1.955 | 0.210-0.260 | H···H | 2.491 | 0.250 | 330 | 36 |
| α-$AlH_3$ | Al-H | 1.726 | 0.361 | H···H | 2.606 | 0.052 | ~100 | 32 |
| α′-$AlH_3$ | Al-H | 1.724 | 0.363 | H···H | 2.707 | 0.043 | ~100 | 45 |
| β-$AlH_3$ | Al-H | 1.726 | 0.364 | H···H | ~2.500 | - | ~100 | 32 |
| γ-$AlH_3$ | Al-H | 1.700-1.778 | 0.328-0.391 | H···H | 2.317-2.623 | 0.037-0.285 | ~100 | 32 |
| $NaAlH_4$ | Al-H | 1.634 | 0.479 | H···H | 2.735-3.086 | 0.026-0.058 | ~230 | 32 |
| $Na_3AlH_6$ | Al-H | 1.804 | 0.332 | H···H | 3.161-3.230 | 0.032 | >265 | 45 |

[†]Experimental topological properties of the electron density obtained from a maximum entropy method (MEM) study.

concepts derived from AIM theory, revealed the presence of a BP and BCP between each hydride ion (Figure 1).[32] Surprisingly, the $\rho_b(\mathbf{r})$ value for these hydride-hydride interactions show that a significant amount of electron density is accumulated in the H···H internuclear region, notwithstanding a long H···H distance of ~2.85 Å (Table 1). In contrast, the increased size of the cations in NaH leads to a larger unit cell, resulting in H···H contacts that exclude the possibility of any such interaction.

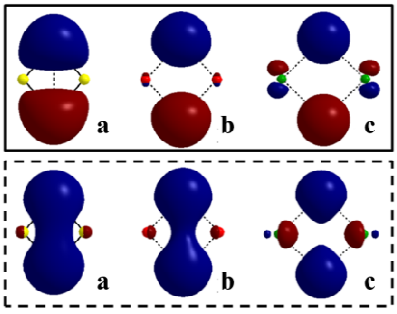


**Figure 2.** Plots of the HOMO (above) and HOMO-1 (below) for the optimised structures of $(LiH)_2$, $(NaH)_2$, and $(KH)_2$, with isoelectronic density levels of 0.337 eÅ$^{-3}$. Reprinted from ref. 33 with the permission of RSC Publishing. Copyright 2014 RSC Publishing.

In order to understand these prototypical binary hydrides in more detail, we carried out a series of CCSD calculations on the rhombic form of salient Group 1 metal hydride dimers $(MH)_2$ (M = Li, Na, and K).[33] This geometry was chosen as a starting point since it closely resembles the smallest repeating unit in the structures of these metal hydrides. Analysis of the HOMO for the optimised structures of these dimers revealed contributions from the *n*s- and *n*p-orbitals of the hydride ions and metal cations, respectively (Figure 2). This is characteristic of a delocalised bonding unit, with the two M-H moieties being mutually connected via bridging hydride ions. The HOMO-1 in these dimers displayed favourable overlap between the two *n*s-orbitals of the hydrides, whereas the compact nature of the 2s orbitals in $(LiH)_2$ resulted in a more diffuse distribution of the density and the formation of a hydride-hydride interaction. Such a scenario is not possible for $(NaH)_2$ and $(KH)_2$, since the corresponding orbitals are defined by smaller and more localised densities. These conclusions are supported by a topological analysis of electron distributions for these dimers.

The desorption of hydrogen from Group 1 metal hydrides is generally assumed to proceed through the simultaneous breaking of the M-H bonds and formation of an H-H moiety.[34] Nevertheless, a topological analysis of the previous $(MH)_2$ dimers revealed a slightly different pathway, in which the M-H bonding was found to initially accumulate electron density as the H···H separation is decreased, signifying a simultaneous strengthening of both of these interactions. However, the stabilising contribution from the cyclic arrangement of these dimers is eventually overwhelmed by the electrostatic repulsion imposed by the hydride-hydride interactions (1.40 Å for Li, 1.70 for Na, and 1.75 for K). At this point on the reaction coordinate there is rapid weakening of the M-H bonding, as the density in the H···H internuclear region becomes more diffuse, giving rise to a more localised distribution in the vicinity of the metal ions. These findings shed new light on the electronic rearrangement necessary for hydrogen evolution, with the cyclic arrangement of the M-H moieties providing the stabilisation necessary to overcome the strong electrostatic repulsion of the H···H interactions on route to the formation of a covalent H-H bond.

The internal energy profiles for the rhombic dimers of LiH-KH also provide a wealth of knowledge concerning the decomposition of Group 1 metal hydrides in the solid state. The larger size of the cations in $(NaH)_2$ and $(KH)_2$ results in an acute H-M-H angle of ~35° at an early stage on their reaction coordinates. This geometry leads to the destabilisation of their cyclic configurations in favour of a linear orientation of the M-H moieties, prior to the liberation of hydrogen (Figure 3).[33] In contrast, the smaller cations in $(LiH)_2$ offer better overlap of the atomic orbitals responsible for the M-H bonding, allowing this dimer to retain its rhombic structure throughout the decomposition process. These findings are consonant with the experimental desorption temperatures of Group 1 metal hydrides (LiH > NaH ≥ KH), as the structural rearrangement

required for the Na and K systems facilitates the release of hydrogen faster than for their Li counterpart.[34] These results also confirm that a strengthening of the hydride-hydride interactions in these systems helps to destabilise their structures and assists in the release of hydrogen.

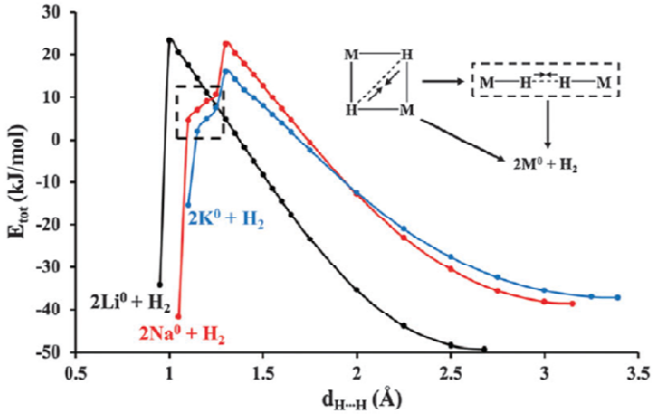


**Figure 3.** Internal energy profiles for the rhombic dimers $(LiH)_2$, $(NaH)_2$, and $(KH)_2$ as they progress towards the release of molecular hydrogen. Reprinted from ref. 33 with the permission of RSC Publishing. Copyright 2014 RSC Publishing.

**3.2 Magnesium Hydrides.** The existence of homopolar dihydrogen bonding in binary hydrides was further revealed for the Group 2 metal hydride β-$MgH_2$, the most stable phase of this system under ambient conditions.[32] This compound crystallises in the rutile lattice *P4₂/mnm* (#136), with the $Mg^{+2}$ cations occupying half the octahedral holes in an hcp array of the hydride ions.[35] This orientation of the atoms gives rise to a distorted rhombic $Mg(\mu\text{-}H)_2Mg$ geometry, similar to that discussed in Section 3.1 for Group 1 metal hydrides, but with an even shorter H···H contact of ~2.50 Å (MH ≥ 2.85 Å).[32] Noritake et al. found that the close approach of these hydride ions resulted in a non-spherical distribution of the density between the two hydridic moieties (Figure 4).[36] Indeed, the experimental $\rho_b(\mathbf{r})$ value for this interaction is nearly identical to the density reported for its more conventional Mg-H bonding (Table 1). This unusual feature led the authors to speculate that this topology may arise from structural defects in the sample, although they did not exclude the possibility of an interaction.

The uncertainty surrounding the surprising build-up of density in the H···H internuclear region of β-$MgH_2$ prompted us to revisit the calculated electronic structure of this binary hydride.[32] This approach provided a means of viewing the subtle details of the chemical bonding in this solid without the complication of structural defects. In this instance, the two bridging hydride ions again interact to accumulate a significant amount of electron density, albeit considerably less than the experimental model ($\Delta\rho_b(\mathbf{r}) = 0.060$ eÅ$^{-3}$).[32,36] Nevertheless, the calculated $\rho_b(\mathbf{r})$ value for this hydride-hydride interaction still constitutes around 70% of the density predicted for the Mg-H bonding in this system (Table 1). This finding not only confirms the presence of homopolar dihydrogen bonding in β-$MgH_2$, but also demonstrates that the strong electrostatic repulsion imposed by the close proximity of these hydride ions does not hinder the formation of an H···H interaction.

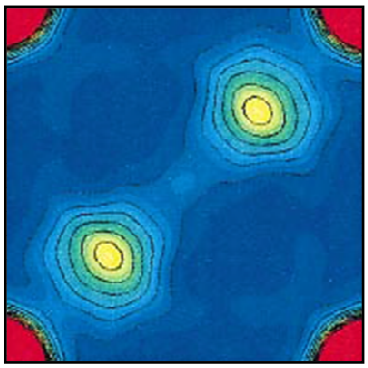

**Figure 4.** Experimental plot of the electron distribution in the H···H internuclear region of β-$MgH_2$. Contours are drawn from 0.0 to 1.5 eÅ$^{-3}$. Reprinted from ref. 36 with permission of AIP Publishing. Copyright 2002 AIP Publishing.

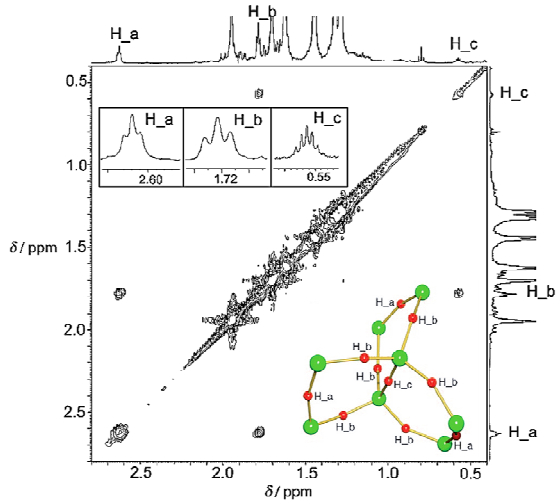


**Figure 5.** $^1H,^1H$-COSY spectrum of $[Mg_8H_{10}]$, along with a ball-and-stick representation of the paddlewheel structure of this cluster. Reprinted from ref. 37 with the permission of Wiley VCH. Copyright 2011 Wiley-VCH.

The identification and characterisation of a hydride-hydride interaction in β-$MgH_2$ represents an important discovery, since a detailed survey of the CSD revealed only eight structures with Mg-H···H-Mg contacts below the sum of van der Waals radii for two interacting hydride ions (2.32-2.80 Å). Remarkably, these interactions exclusively involve bridging hydride ions resulting primarily in the formation of $Mg(\mu\text{-}H)_2Mg$ moieties that closely resemble the structural motifs observed in the previous binary hydrides.[32,36] However, an Mg-H cluster containing a paddlewheel $[Mg_8H_{10}]$ core was also found to exhibit relatively short H···H contacts (>2.57 Å) between neighbouring hydride ions.[37] In this instance, the bulky organic ligands that protect the Mg-H core allowed the structure of this system to be retained in aprotic solvents. This permitted a means of measuring the $^1H,^1H$ COSY spectrum of the material,

which presented hydride-hydride coupling within the $[Mg_8H_{10}]$ framework (Figure 5).[37] Unfortunately, the authors were uncertain whether this coupling was the result of a through-bond or through-space interaction.

In the solid-state, the $[Mg_8H_{10}]$ cluster was shown to evolve a significant amount of hydrogen at ~200 °C, considerably lower than bulk β-$MgH_2$ (~330 °C).[34,37] This enhanced reactivity prompted Harder et al. to further explore the relationship between the size of Mg-H clusters and their hydrogen release properties.[38,39] The authors found that smaller $[Mg_nH_m]$ fragments led to the release of hydrogen at lower temperatures, consistent with previous calculation on related Mg-H complexes (Scheme 2).[40] Interestingly, the hydride-hydride coupling in these systems displayed the opposite trend, with increasing coupling as the cluster size decreased: $[Mg_2H_2]$ > $[Mg_4H_4]$ > $[Mg_8H_{10}]$. This preliminary correlation suggests that hydride-hydride interactions may play a key role in influencing the thermal behaviour of these clusters. Indeed, a decrease in the H···H distance results in an increased coupling constant, with no apparent relation to the Mg-H bonding. However, this trend seems to be exclusive to these clusters, as β-$MgH_2$ decomposes at a higher temperature and displays a shorter H···H contact (~2.50 Å) than the two largest $[M_nH_m]$ moieties.

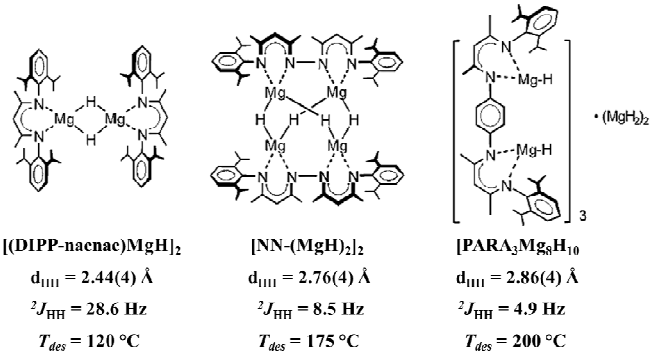


**Scheme 2.** Plot of a series of $[Mg_nH_m]$ clusters with their H···H distances, $^1H,^1H$ coupling constants, and hydrogen desorption temperatures. Modified from ref. 39 with the permission of Wiley VCH. Copyright 2014 Wiley-VCH.

**3.3 Boron Hydrides.** The structural chemistry of boranes has been of considerable interest for more than half a century, owing to the elaborate B-B and B-H-B bonding exhibited by these systems.[41] diborane contains a bridging B(μ-H)$_2$B moiety, analogous to the structural motif observed for the metal hydrides discussed in Section 3.1 and 3.2.[32,42] This geometry results in a remarkably short H···H separation of 1.76 Å for the bridging hydrogen atoms, although the calculated density shows no evidence of any bonding interaction (Figure 6).[32] In contrast, a significant amount of electron density is accumulated in the H···H internuclear region of the related calculated $Al_2H_6$ dimer. This difference may be attributed to the more diffuse and polarisable electron distribution in the Al derivative, which encourages the formation of a homopolar dihydrogen bond. However, $Al_2H_6$ has no existence as a discrete molecular entity (q.v.). Although $B_2H_6$ lacks an intramolecular H···H interaction, the extended structure of this compound in the solid state is stabilised through supramolecular interactions between bridging and terminal hydrides of neighbouring entities (>2.72 Å).[42]

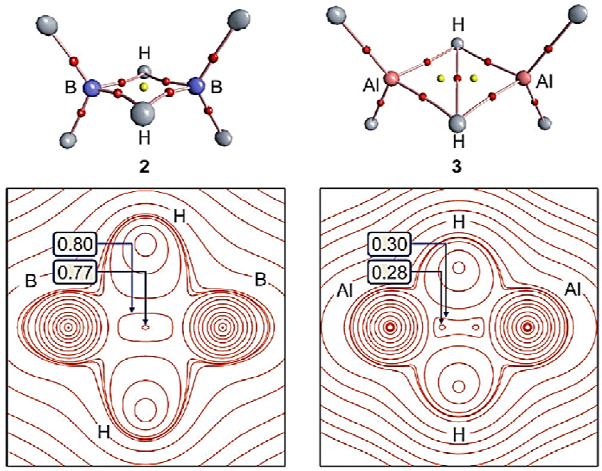


**Figure 6.** Molecular graph for the calculated structure of $B_2H_6$ and $Al_2H_6$ displaying the BPs and BCPs (red spheres) in these dimers. Contour plots of the $H_2E(\mu\text{-}H)_2EH_2$ plane of these molecules with lines drawn at 2, 4, and 8 x $10^{-n}$ eÅ$^{-3}$ (n = -3, -2, -1, 0, 1, 2) with extra lines at 0.70, 0.77, 0.90, 1.3 (for B) and 0.28, 0.30 (Al) eÅ$^{-3}$. Reprinted from ref. 32 with the permission of Wiley VCH. Copyright 2012 Wiley-VCH.

In order to explore the prevalence of hydride-hydride interactions in the structures of boranes we conducted a survey of the CSD for both neutral and anionic $B_xH_y$ complexes, with B-H···H-B contacts ranging from 2.0-2.8 Å. This revealed over 1300 structures (omitting systems containing transition metals), with an average H···H distance of 2.62 Å. These homopolar dihydrogen contacts are often in competition with more conventional interactions, such as M···H-B bonding, but also act as the exclusive means of stabilising many neutral $B_xH_y$ structures (*e.g.* $B_5H_9$, $B_5H_{11}$). This analysis provides compelling evidence of the role played by homopolar hydrogen bonding in the structural chemistry of these hydrogen-rich materials. The unusual ability of B-H moieties to engage in hydride-hydride interactions is discussed in more detail for metal borohydrides (Section 3.5) and B-N-H compounds (Section 4.0).

**3.4 Aluminum Hydride.** The final binary hydride to be discussed in this section is $AlH_3$, which is capable of crystallising in at least seven different polymorphs.[43] The most stable phase of this hydride adopts a rhombohedral cell in the trigonal space group *R-3c* (#167), α-$AlH_3$.[44] This structure consists of corner-sharing $AlH_6$ octahedra connected through bridging hydride ions (Figure 7a).[32,44] A topological analysis of α-$AlH_3$ revealed the presence of a weak hydride-hydride interaction (2.606 Å) that serves as an additional cross-link in the network of corner-sharing $AlH_6$ octahedra (Figure 7b). The calculated $\rho_b(\mathbf{r})$ value for this H···H interaction is relatively low compared to the homopolar dihydrogen bonding observed in

related binary hydrides (Table 1). For example, the hydride-hydride interaction in the structure of β-$MgH_2$ is only 0.1 Å shorter, but accumulates nearly three times the amount of density as its counterpart in α-$AlH_3$ (0.08 eÅ$^{-3}$). Nevertheless, the topological characteristics of this H···H interaction still fall within the realm of weak proton-hydride bonding, and their high multiplicity (six per unit cell) suggests that these interactions contribute to the stability of the extended structure.[32,45]

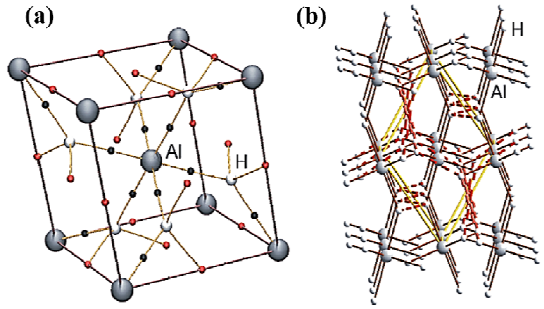


**Figure 7.** (a) Molecular graph for the calculated rhombohedral unit cell for α-$AlH_3$, with the H···H and M-H BCP denoted as solid red and black spheres, respectively. (b) Plot of the H···H interactions (dashed red lines) in the structure of α-$AlH_3$. Reprinted from ref. 32 with the permission of Wiley VCH. Copyright 2012 Wiley-VCH.

The α′-phase of $AlH_3$ adopts the orthorhombic space group *Cmcm* (# 63) and consists of corner-sharing $AlH_6$ octahedra.[46] This packing motif leads to interconnected ion pairs that create large cavities throughout the cell (diameter of 4.18 Å). A preliminary topological analysis of this structure identified a hydride-hydride interaction (2.707 Å) that accumulates a similar amount of electron density as its α-$AlH_3$ polymorph.[47] The β-phase of $AlH_3$ crystallises in the cubic space group *Fd-3m* (#227), adopting a structure that closely resembles its α′-$AlH_3$ counterpart.[48] However, the corner-sharing $AlH_6$ octahedra in α′-$AlH_3$ result in smaller channels (diameter of 3.90 Å), with a much shorter H···H contact of 2.5 Å. Remarkably, no appreciable amount of density was observed between these two hydride ions.[32] The thermal decomposition of these two polymorphs of $AlH_3$ proceeds in each case through an exothermic transition to α-$AlH_3$ above 100 °C if the heating rate is slow, but they can release hydrogen directly without this phase change at lower temperatures.[43] Such complicated behaviour is dictated by the kinetics of the various processes involved, preventing meaningful correlations between the structures of these systems and their desorption temperatures.

The least stable phase of the four primary polymorphs of this binary hydride is γ-$AlH_3$, which crystallises in the orthorhombic space group *Pnnm* (#58).[49] The structure of γ-$AlH_3$ consists of both corner- and edge-sharing $AlH_6$ octahedra, giving rise to a chain-like arrangement of these moieties. The edge-sharing octahedra result in two $Al^{+3}$ cations being mutually connected via a pair of bridging hydride ions, in a manner analogous to the M(μ-H)$_2$M motifs observed in the previous binary hydrides. Figure 8 shows that the hydride ions in γ-$AlH_3$ are highly polarised towards the $Al^{+3}$ cations. However, this feature does not hinder the formation of a short hydride-hydride interaction of 2.317 Å, which accumulates more than twice the density observed in its $Mg^{+2}$ counterpart (Table 1).[32] Remarkably, the calculated $\rho_b(\mathbf{r})$ value for this H···H interaction constitutes approximately 80% of the density predicted for the Al-H bonding. The extended structure of γ-$AlH_3$ is then supported by weak H···H interactions (2.623 Å) that connect the corner- and edge-sharing $AlH_6$ octahedra. These latter hydride-hydride interactions are characterised by only a small fraction of the density found in the Al(μ-H)$_2$Al region, but are of comparable strength to the related interactions found in the other polymorphs of $AlH_3$ (Table 1).

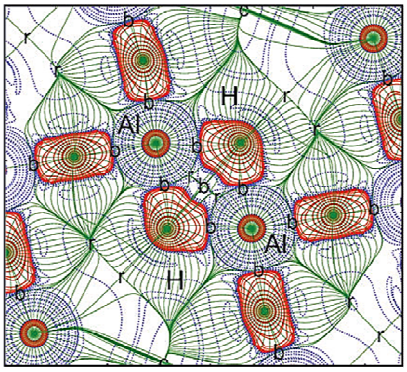


**Figure 8.** Contour plots of the negative Laplacian of the electron density, $-\nabla^2\rho(\mathbf{r})$, in the Al(μ-H)$_2$Al region of **γ-5**. Solid and dashed lines represent charge concentration and depletions, repectively. Reprinted from ref. 32 with the permission of Wiley VCH. Copyright 2012 Wiley-VCH.

**3.5 Complex Metal Hydrides.** The ubiquitous nature of homopolar dihydrogen bonding in binary hydrides prompted us to extend our topological analysis to $NaAlH_4$, one of the most widely studied hydrogen storage materials.[50] This hydride crystallises in the tetragonal space group *I4$_1$/a* (#88), in which the isolated $[AlH_4]^-$ tetrahedra engage in a multitude of stabilising Na···H-Al interactions (2.439-2.456 Å).[51] This results in a distorted antiprismatic geometry for the $Na^+$ cations, in which the $\rho_b(\mathbf{r})$ values for the Na···H-Al interactions are similar to their Na···H···Na counterparts in NaH ($\Delta\rho_b(\mathbf{r}) \sim 0.025$ eÅ$^{-3}$).[32] In addition, the hydride ions also engage in a plethora of weak hydride-hydride interactions (Table 1) that serve as cross-links between adjacent $[AlH_4]^-$ moieties, analogous to the structural motifs found for the $AlH_3$ polymorphs. These H···H interactions accumulate only a modest amount of electron density, but their multiplicity (40 per unit cell) indicates that a significant amount of density is redistributed within the H···H internuclear regions of this complex metal hydride.

$$NaAlH_{4\,(s)} \rightarrow {}^1/_3\, Na_3AlH_{6\,(s)} + {}^2/_3Al_{\,(s)} + H_{2\,(g)} \qquad (1)$$

$$Na_3AlH_{6\,(s)} \rightarrow 3NaH_{\,(s)} + Al_{\,(s)} + {}^3/_2\, H_{2\,(g)} \qquad (2)$$

The release of hydrogen from $NaAlH_4$ occurs through a two-step process, giving rise to the intermediate $Na_3AlH_6$, which subsequently decomposes further to NaH (Eqs. 1-2).[29] The number of hydride-hydride interactions in $NaAlH_4$

prompted us also to carry out a topological analysis of its primary decomposition product $Na_3AlH_6$. The perovskite-type structure of this system was found to fit most closely the monoclinic space group $P2_1/n$ (#14), with the $Na^+$ cations occupying all the octahedral and tetrahedral holes in an fcc array of $[AlH_6]^{3-}$ anions.[52] The extended structure of $Na_3AlH_6$ is then stabilised by Na···H-Al interactions (2.226-2.766 Å), which accumulate a similar amount of density as their counterparts in $NaAlH_4$.[47] However, the secondary H···H interactions in $Na_3AlH_6$ are characterised by smaller $\rho_b(\mathbf{r})$ values, with a substantial decrease in their multiplicity (4 per unit cell). These findings suggest that hydride-hydride interactions gradually weaken and become less frequent as $NaAlH_4$ proceeds through its decomposition reactions. Such a trend offers an attractive means of viewing the overall hydrogen release process, but it is dangerous to infer too much from the limited number of systems available in our analysis, as other crystal packing energies and M···H-X bonding will also contribute significantly to the overall thermal behaviour of these hydrogen storage materials.

The proclivity of complex metal hydrides to form H···H interactions in the solid-state was further revealed from a survey of the CSD, in which over 40 structures containing $[BH_4]^-$ anions were found to possess H···H distances below the sum of the van der Waals radii for two interacting hydride ions. For example, $Be(BH_4)_2$ crystallises in the tetragonal space group $I4_1cd$ (#110), with Be···H-B resulting in polymeric helical chains that run along the ac plane of the crystal.[53] This leaves the $Be^{2+}$ ions saturated with only secondary hydride-hydride interactions (2.727-2.851 Å) to stabilise the remaining dimensions of the solid (Figure 9a). This situation closely resembles the structures of layered *n*-alkanes, in which weak dispersion forces or C-H···H-C interactions serve as the primary stabilising force in these systems (Figure 9b).[54]

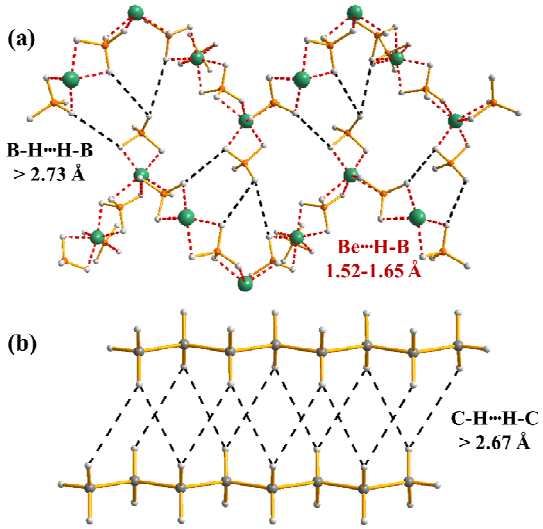


**Figure 9.** Plot of the homopolar dihydrogen bonding in the extended structures of (a) $Be(BH_4)_2$ and (b) $CH_3(CH_2)_6CH_3$.

Our CSD survey also showed that under appropriate conditions, homopolar dihydrogen bonding can serve as the primary stabilising interaction in certain systems. This is clearly illustrated for $Hf(BH_4)_4$, which adopts the cubic space group *P-43m* (#215).[55] The higher oxidation state of the metal centre relative to its Be counterpart leads to a distorted tetrahedral orientation of the $[BH_4]^-$ moieties. This geometry prevents the formation of any additional Hf···H-B interactions (Figure 10a), leaving only the terminal B-H bonds to engage in stabilising B-H···H-B interactions. Accordingly, the extended structure of $Hf(BH_4)_4$ consists of an elaborate network of weak hydride-hydride interactions (>2.637 Å), which hold the crystalline framework together (Figure 10b). These weak intermolecular interactions represent the sole mechanism available for the stabilisation of crystalline $Hf(BH_4)_4$, in a scenario analogous to the condensation of gases like argon and nitrogen, and are consistent with the high volatility of the compound at ambient temperatures.[56,57] The ability of homopolar dihydrogen bonding to stabilise the extended structures of volatile molecular species such as $Hf(BH_4)_4$ further demonstrates that mutual polarisation of the hydride ions leads to a structurally significant van der Waals attraction.

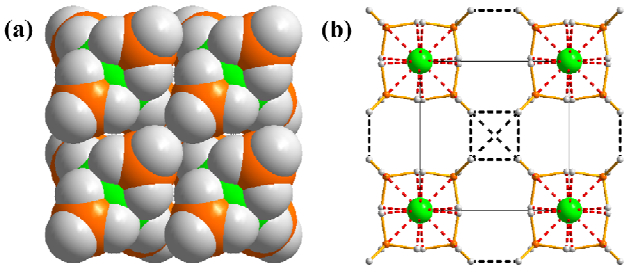


**Figure 10.** (a) Space-filling diagram of cubic structure of $Hf(BH_4)_4$ and (b) a plot of the weak B-H···H-B bonding in $Hf(BH_4)_4$. The Hf···H-B/Hf···B and B-H···H-B interactions are denoted as red and black dashed lines, respectively.

## 4. Homopolar *vs.* Heteropolar Dihydrogen Bonding

Amine boranes and their derivatives have attracted a considerable amount of attention in recent years as chemical hydrogen storage materials. They have also served as the benchmark systems in the discovery and characterisation of N-H····H-B proton-hydride interactions in the solid state.[58] These heteropolar dihydrogen bonds were long presumed to be the sole driving force behind the evolution of hydrogen from amine boranes.[59] However, the large number of hydridic B-H moieties present in these compounds also affords the possibility of hydride-hydride interactions, analogous to the borohydride systems discussed in Section 3.5. In the following sections we will explore the prevalence of homopolar dihydrogen bonding in this class of chemical hydrides, and their potential involvement in the liberation of hydrogen from these systems.

**4.1 Molecular Hydrides.** The structure and reactivity of amine-borane adducts is largely dependent on their ability to engage in N-H····H-B proton-hydride interactions. This is exemplified for ammonia borane, $NH_3BH_3$, in which the oppositely charged hydrogen atoms on the boron and nitrogen

atoms offer a direct and straightforward pathway for the release of hydrogen.[60] However, Autrey et al. demonstrated that the decomposition of $NH_3BH_3$ occurs through a more complex process:[61] *in situ* $^{11}B$ NMR experiments showed that disruption of the proton-hydride interactions during the induction period leads to the formation of the isomeric diammoniate of diborane, $[NH_3BH_2NH_3]^+[BH_4]^-$. This mobile isomer then reacts with $NH_3BH_3$ to liberate hydrogen through a bimolecular process, as shown in Eq. 3 and 4.

$$2\ NH_3BH_{3\ (s)} \leftrightarrow [NH_3BH_2NH_3]^+[BH_4]^-_{\ (g)} \quad (3)$$

$$[NH_3BH_2NH_3]^+[BH_4]^-_{\ (s)} + NH_3BH_{3\ (s)} \rightarrow [NH_2BH_2]_{n\ (s)} + nH_{2\ (g)} \quad (4)$$

A detailed analysis of the solid-state structures of these and other B-N-H compounds should afford a better understanding of this complex reaction pathway. Crystalline $NH_3BH_3$ adopts the orthorhombic space group $Pmn2_1$ (#31) at low temperatures,[62] resulting in short N-H···H-B contacts (2.02-2.22 Å) that represent the sole means of stabilising the extended structure of this system. At room temperature, a phase transition occurs to a tetragonal cell (*I4mm*; #107), in which the crystallographic symmetry gives rise to a disordered array of hydrogen atoms.[63] This geometry also facilitates the formation of short proton-hydride interactions (~1.91 Å), and neutron diffraction experiments and molecular simulations suggest that these are weakened in the higher temperature phase.[64] In contrast, the conversion of $NH_3BH_3$ to its isomeric form $[NH_3BH_2NH_3]^+[BH_4]^-$ leads to a strengthening of N-H···H-B bonding (1.80-2.36 Å).[65] The strength and number of N-H···H-B interactions in these two isomeric amine-boranes clearly illustrates how these materials are capable of releasing hydrogen through a proton-hydride reaction pathway.

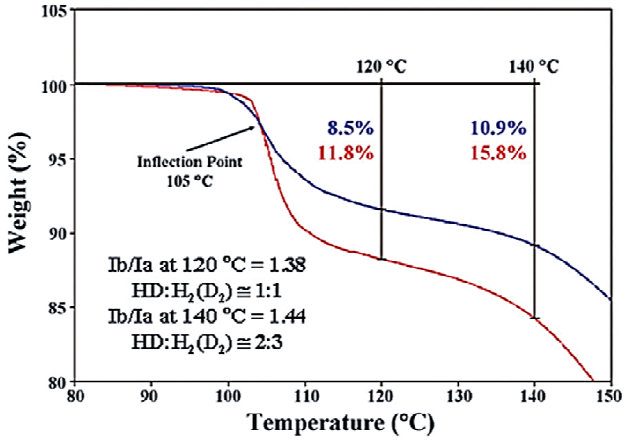


**Figure 11.** TGA plot for the thermal evolution of hydrogen from $ND_3BH_3$ (blue) and $NH_3BD_3$ (red), illustrating the significant contribution from hydride-hydride interactions. Reprinted from ref. 66 with the permission of RSC Publishing. Copyright 2012 RSC Publishing.

The shortest B-H···H-B contacts in these two structures are 3.05 Å for $NH_3BH_3$ and 2.80/2.99 Å for $[NH_3BH_2NH_3]^+[BH_4]^-$, which appears to preclude their involvement in the thermal release of hydrogen. However, our recent investigation of two selectively-labelled isotopomers of $NH_3BH_3$ ($NH_3BD_3$ and $ND_3BH_3$) showed conclusively that a significant amount of hydrogen is evolved thermally via a hydride-hydride pathway.[66] Thermogravimetric analysis (TGA) demonstrated that N-H···H-B and B-H···H-B desorption pathways contribute nearly equal amounts of hydrogen below 120 °C, with the hydride-hydride pathway becoming more dominant after the solid has melted and the molecules become mobile (Figure 11). This conclusion was corroborated by $^1H$ and $^2H$ NMR experiments, with both HD (*i.e.* N-H···H-B pathway) and $H_2/D_2$ (*i.e.* B-H···H-B pathway) being observed in 1:1 ratios for the first stage of these reactions (< 120 °C). *In situ* Raman spectroscopy studies of the isotopomers showed no evidence of H/D scrambling prior to hydrogen evolution.[67] This important study shows that hydride-hydride interactions can effectively compete with more conventional pathways, to play a significant role in the evolution of hydrogen from molecular hydrides.

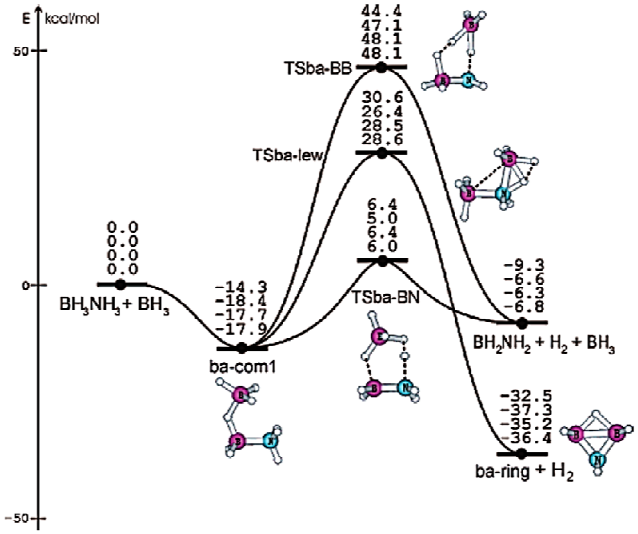


**Figure 12.** Schematic energy profiles for the $BH_3$-catalysed dehydrogenation of $NH_3BH_3$, with relative energies in kcal/mol. Reprinted from ref. 69 with the permission of American Chemical Society. Copyright 2007 American Chemical Society.

Computational methods have also provided important mechanistic insights into the thermal behaviour of $NH_3BH_3$. Early studies by Zhang et al. predicted a large kinetic barrier for the loss of the first equivalent of hydrogen (~138 kJ/mol).[68] However, Dixon et al. found that the dissociation energies for $NH_3BH_3$ were lower than previously proposed when free $BH_3$ is incorporated into the calculations, as this Lewis acid can act as a catalyst in the dehydrogenation.[69] This pathway was later supported by Shore et al., who showed that in solution $BH_3$ can mediate the release of hydrogen from $NH_3BH_3$.[70] The calculated reaction for $NH_3BH_3{\cdot}BH_3$ may proceed through three possible routes (Figure 12). The lowest energy pathway involves the expected formation of a N-H···H-B proton-hydride interaction (~6.4 kcal/mol), whereas the highest transition state proceeds through homopolar dihydrogen bonding (~48.1

kcal/mol). While gas-phase calculations like these can provide important insights into key interactions and their interrelationship, they are unable to account for solid-state contributions to the process for compounds like $NH_3BH_3$, which may bring the hydride-hydride pathway closer in energy to its more proton-hydride counterpart as the hydrogen release coordinate is traversed.

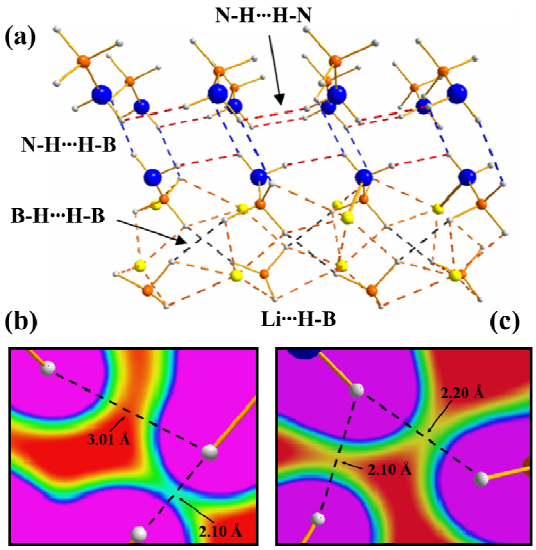


**Figure 13.** (a) Plot of the extended structure of $LiNH_2BH_3$ with the Li···H-B, N-H···H-B, and B-H···H-B interactions denoted as dashed orange, blue, and black lines, respectively. Calculated valance electron density plots for select (b) B-H···H-B and (c) N-H···H-B interactions in $LiNH_2BH_3$. Contour levels increase from 0.03 (red) to 0.05 (yellow) to 0.07 (green) to 0.09 (blue) to 0.11 (dark blue) to 0.14 (purple) eÅ$^{-3}$. Reprinted from ref. 72 with the permission of American Chemical Society. Copyright 2011 American Chemical Society.

**4.2 Metal Amidoboranes.** The prototypical amidoboranes $LiNH_2BH_3$ and $NaNH_2BH_3$ each crystallise in the orthorhombic space group *Pbca* (#61), with the $M^+$ ions adopting a pseudo-tetrahedral orientation of the $[NH_2BH_3]^-$ anions.[71] This geometry results in the formation of 2D polymeric arrays that are stabilised primarily by M···H-B interactions (Figure 13a). The various layers of the solid are then connected through N-H····H-B proton-hydride bonding (2.21-2.56 Å). However, closer inspection of $LiNH_2BH_3$ also reveals short H···H contacts (2.11 Å) between neighbouring B-H moieties.[72] Analysis of the calculated valence electron density in the vicinity of this hydride-hydride interaction clearly shows that a significant amount of electron density is accumulated in this region (Figure 13b). The $\rho_b(\mathbf{r})$ value for this interaction is comparable with the Li···H-B bonding in $LiNH_2BH_3$ (Table 2) and is nearly twice the value observed for its more conventional N-H····H-B counterpart (Figure 13c). In contrast, the larger size of the $Na^+$ ions in $NaNH_2BH_3$ results in weaker dispersion forces and less density being accumulated within the H···H internuclear region. Nevertheless, these findings suggest that homopolar dihydrogen bonding may also play a role in the release of hydrogen from these $MNH_2BH_3$ systems.

**Table 2.** Topological properties of the electron density for the calculated M···H-B and H···H interactions in salient $MNR_2BH_3$ compounds.[72,77]

| Compound | Interaction | Distance | $\rho_b(r)$ |
|---|---|---|---|
| $LiNH_2BH_3$ | Li···H-B | 2.02-2.13 | 0.058-0.105 |
| | N-H···H-B | 2.20-2.59 | 0.029-0.057 |
| | B-H···H-B | 2.10-2.83 | 0.031-0.091 |
| $NaNH_2BH_3$ | Na···H-B | 2.54-2.60 | 0.046-0.051 |
| | N-H···H-B | 2.75-3.15 | 0.009-0.020 |
| | B-H···H-B | 2.96-3.38 | 0.011-0.021 |
| $LiNMe_2BH_3$ | Li···H-B | 1.97-2.13 | 0.100 |
| | N-H···H-B | - | - |
| | B-H···H-B | 2.56 | 0.060 |

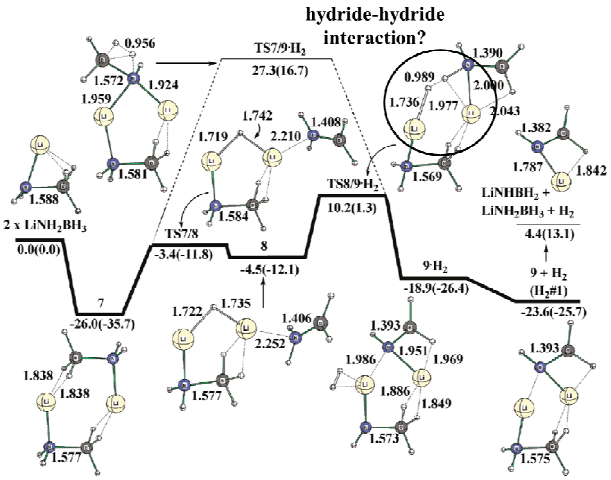


**Figure 14.** Free energy surface for the dehydrogenation of $LiNH_2BH_3$. Reprinted from ref. 74 with the permission of American Chemical Society. Copyright 2009 American Chemical Society.

The substitution of a protic hydrogen atom on the $NH_3$ moiety of $NH_3BH_3$ by a more electropositive alkali metal has a pronounced impact on the thermal behaviour of the resulting $MNH_2BH_3$ derivatives.[73] The shift from a molecular to an ionic framework often leads to enhanced hydrogen release properties and suppression of unwanted volatile by-products. This feature has prompted considerable experimental and computational efforts direct at elucidating the reaction mechanism for these hydrogen storage candidates.[74,75] McKee et al. predicted a two-step process for the release of hydrogen from $LiNH_2BH_3$, in which the initial transition state consisted of a bridging Li···H···Li moiety bound to a dehydrogenated $NH_2$=$BH_2$ fragment (Figure 14).[74] The bridging hydride ion then interacts with the $NH_2$=$BH_2$ moiety to liberate the first equivalent of hydrogen. This process appears to proceed through an intermediate state that involves the transfer of a protic hydrogen atom of the $NH_2$=$BH_2$ group to the Li···H···Li moiety giving rise to a hydride-hydride interaction (*i.e.* Li-H···H-Li).

More recently, Luedtke and Autrey explored the reaction rates for the thermal decomposition of $LiNH_2BH_3$ using its partially deuterated isotopomers.[76] These authors found that $LiND_2BH_3$ releases 0.5 equivalent of hydrogen at the same rate as its non-deuterated counterpart, whereas the stronger B-D bonds in $LiNH_2BD_3$ gave rise to a much slower reaction. These findings suggest that the rate-determining step in this process is the scission of the B-H(D) bonds. The difference in reactivity of these isotopomers led us to explore the potential contribution of a hydride-hydride pathway for $LiNH_2BH_3$, using similar $^1H$ NMR experiments employed for $NH_3BH_3$ (Section 4.1).[66,72] Staged heating of an $LiND_2BH_3$ sample to 140 °C resulted in the appearance of both HD and $H_2$ in a 1:2 ratio (Figure 15). This study shows that an N-H···H-B pathway still dominates the evolution of hydrogen, but with an appreciable contribution also from a hydride-hydride release mechanism.

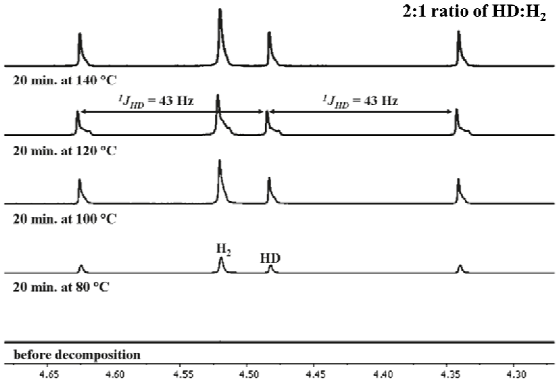


**Figure 15.** $^1H$ NMR spectra ($d_8$-toluene) of the hydrogen isotopomers evolved from heating a sample of $LiND_2BH_3$. Reprinted from ref. 72 with the permission of American Chemical Society. Copyright 2011 American Chemical Society.

The ubiquitous nature of homopolar dihydrogen bonding was further revealed in the structure of $LiNMe_2BH_3$, which crystallises in the monoclinic space group $P2_1/c$ (#14).[77] In this instance, the dominant Li···H-B interactions give rise to 1D polymeric chains that draw several B-H moieties into close enough proximity to facilitate B-H···H-B contacts of 2.43 Å. This bonding motif closely resembles the zig-zag pattern of the hydride-hydride interactions found in the polymeric layers of $LiNH_2BH_3$. However, a topological analysis of $LiNMe_2BH_3$ showed that this H···H interaction accumulates only a fraction of the density reported for its counterpart in $LiNH_2BH_3$. This difference can potentially be attributed to the near-linear disposition of the B-H bonds in the fully protonated derivative, whereas the B-H···H-B contacts in $LiNMe_2BH_3$ adopt a bent orientation of the B-H moieties. A statistical survey of the CSD demonstrated that these B-H···H-B interactions display a clear angular dependence, analogous to the more conventional N-H···H-B proton-hydride bonding (Figure 16).[12] The B-H···H angles cluster between 95 and 180°, illustrating the ability of the B-H moiety to engage in both bent and linear interactions. These findings illustrate how homopolar dihydrogen bonding accommodate or compete with more conventional interactions such as proton-hydride bonding in directing the structure and reactivity of a wide range of hydrogen-rich materials.

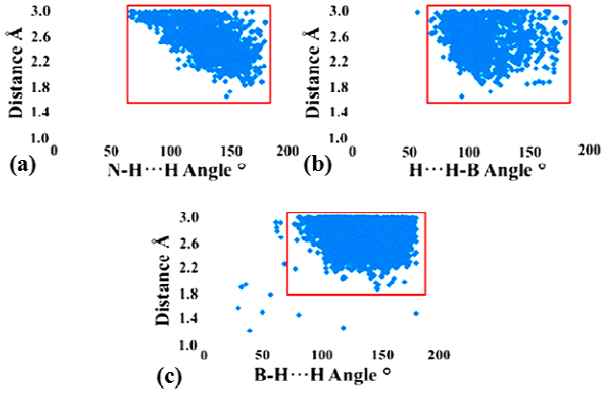


**Figure 16.** CSD survey of the angle dependence for (a/b) N-H···H-B contacts (1135 hits) and (c) B-H···H-B contacts (7441 hits). Reprinted from ref. 77 with the permission of American Chemical Society. Copyright 2011 American Chemical Society.

The solid-state structures of $MNMe_2BH_3$ (M = Li and K) compounds also point to a supramolecular application for homopolar dihydrogen bonding.[77] In these instances, the primary M···H-B interactions result in 1D or 2D polymeric arrays, while the methyl groups of the amine portion of the anions are oriented to form a multitude of weak C-H···H-C interactions. These structural motifs are again reminiscent of the previously described layered *n*-alkanes (Section 3.5), and highlight an important role in the design of soft molecular materials, such as liquid crystals and inorganic polymers. Indeed, a number of silane derivatives form similar Si-H···H-Si interactions to stabilise their extended structures. For example, the structure of the organosilane dendrimer tetrakis(tris(silylethyl)silylethyl)silane can only be stabilised in the solid state through Si-H···H-Si interactions.[78]

## 5. Summary and Outlook

The aim of this perspective has been to provide a detailed account of recent advances in our understanding of homopolar dihydrogen bonding, and an appreciation of its effects on the structure and reactivity of hydrogen-rich materials. The vast majority of solid-state hydrogen storage materials adopt structural motifs that bring two M-H moieties into close enough proximity to facilitate hydride-hydride interactions of the sort discussed here. This is clearly evident for Group 1 and 2 binary hydrides, which generally contain bridging hydride ions that form stabilising $M(\mu\text{-}H)_2M$ motifs. Such a geometry allows the highly polarisable hydride ions to share a significant amount of electron density in the H···H internuclear region, with $\rho_b(\mathbf{r})$ values as high as 70% of the density observed for the corresponding M-H bonds. Modelling the hydrogen release pathways for rhombic dimers of alkali metal hydrides has shown that the electrostatic repulsion imposed in this geometry is overcome through the cyclisation of the M-H bonds, as a

strengthening of the H···H bonding destabilises the M(μ-H)$_2$M framework and results in the release of hydrogen.

Our analysis of homopolar dihydrogen bonding in metal amidoborane derivatives $MNR_2BH_3$ revealed that these interactions are capable of competing effectively with more conventional ones in redistributing electron density throughout the crystalline framework. This is best illustrated for the B-H···H-B interactions trapped within the polymeric layers of $LiNH_2BH_3$. Here the hydride-hydride interactions accumulate a comparable amount of density as their Li···H-B counterparts, and nearly twice the amount predicted for the N-H···H-B proton-hydride bonding in this system. Isotopic labelling studies showed that a significant fraction of hydrogen released from this material also originates from a B-H···H-B source, in contrast to previous notions that the process exclusively occurs through a proton-hydride pathway. Remarkably, a similar hydride-hydride reaction coordinate was observed for its parent compound $NH_3BH_3$, in spite of the absence of any short B-H···H-B interactions in the solid-state. This pathway becomes more dominant upon melting, consistent with the increased mobility enjoyed by the molecule in the liquid phase.

The number of solid-state hydrogen storage materials that have now been shown to contain hydride-hydride interactions attests to their central importance in the chemistry of these systems. However, this counter-intuitive bonding motif also represents a convenient means for stabilising low-dimensional materials and the condensed phases of metal hydrides, analogous to the intermolecular interactions responsible that support the crystal structures of $Be(BH_4)_2$ and $Hf(BH_4)_4$. In such instances saturation of the metal centre by conventional M···H-B bonding leaves only weak secondary hydride-hydride interactions to hold together the supramolecular structure of the solid. The intermolecular bonding in solids like these closely resembles London dispersion forces, with a repulsive (first-order) electrostatic interaction being overcome by the attractive (second-order) induced dipole moment that arises from polarisation of the electron density. We anticipate that homopolar H···H interactions may also be widespread in the structural chemistry of transition metal hydrides, especially since many such systems display M(μ-H)$_2$M moieties similar to their main group counterparts discussed here.[79] This bonding motif may then play an important role in key catalytic reactions like metathesis and transfer hydrogenation.

## Acknowledgements

We are grateful to the National Sciences and Engineering Research Council of Canada (NSERC) and New Brunswick Innovation Foundation (NBIF) for financial support of the work conducted throughout this Perspective.

## Notes and references

*Department of Chemistry, University of New Brunswick, P.O. Box 4400, Fredericton, N.B., Canada, E3B 5A3, e-mail:* dwolsten@unb.ca *and* smcgrady@unb.ca

1 T.S. Moore and T.F. Winmill, *J. Chem. Soc.*, 1912, **101**, 1635-1676.

2 G.A. Jeffrey, *An Introduction to Hydrogen Bonding*, Oxford University Press, Oxford, 1997.

3 G.R. Desiraju and T. Steiner, *The Weak Hydrogen Bond in Structural Chemistry and Biology*, Oxford University Press, New Work, 1999

4 S.J. Grabowski, *Chem. Rev.*, 2011, **111**, 2597-2625.

5 L. Pauling, *J. Am. Chem. Soc.*, 1931, **53**, 3225-3237.

6 L. Pauling, *The Nature of the Chemical Bond*, 3rd d., Cornell University Press, Ithaca, N.Y., 1960.

7 G.N. Lewis, *Valence and Structure of Atoms in Molecules*, Chemical Catalog Co., New York, 1923.

8 G.C. Pimentel and A.L. McClellan, *The Hydrogen Bond*, W.H. Freeman and Co., San Francisco and London, 1960.

9 O. Takahashi, Y. Kohno, and M. Nishio, *Chem. Rev.*, 2010, **110**, 6049-6076.

10 R. Custelcean and J.E. Jackson, *Chem. Rev.*, 2001, **101**, 1963-1980.

11 (a) M.P. Brown and R.W. Heseltine, *Chem. Commun.*, 1968, 1551-1552; (b) M.P. Brown, R.W. Heseltine, P.A. Smith, and P.J. Walker, *J. Chem. Soc. A*, 1970, 410-414.

12 T.B. Richardson, S. de Gala, R.H. Crabtree, and P.E.M. Siegbhan, *J. Am. Chem. Soc.*, 1995, **117**, 12875-12876.

13 S.J. Grabowski, *Chem. Phys. Lett.*, 1999, **312**, 542-547.

14 S.J. Grabowski, *J. Phys. Chem. A*, 2000, **104**, 5551-5557.

15 J.C. Lee, A.L. Rheingold, B. Muller, P.S. Pregosin, and R.H. Crabtree, *J. Chem. Soc., Chem. Commun.*, 1994, 1021-1022.

16 (a) A.J. Lough, S. Park, R. Ramachandran, and R.H. Morris, *J. Am. Chem. Soc.*, 1994, **116**, 8356-8357; (b) S. Park, R. Ramachandran, A.J. Lough, and R.H. Morris, *J. Chem. Soc., Chem. Commun.*, 1994, 2201-2202.

17 Q. Liu and R. Hoffmann, *J. Am. Chem. Soc.*, 1995, **117**, 10108-10112.

18 L.M. Epstein, E.S. Shubina, *Coord. Chem. Rev.*, 2002, **231**, 165-181.

19 V.I. Bakhmutov, *Dihydrogen Bond: Principles, Experiments, and Applications*, John Wiley & Sons, New Jersey, 2008.

20 (a) G.S. McGrady and G. Guilera, *Chem. Soc. Rev.*, 2003, **32**, 383-392; (b) C.A. Sandoval, T. Ohkuma, K. Muñiz, and R. Noyori, *J. Am. Chem. Soc.*, 2003, **125**, 13490-13503; (c) T. Li, I. Bergner, F.N. Haque, M. Zimmer-De Iuliis, D. Song, and R.H. Morris, *Organometallics*, 2007, **26**, 5940-5949.

21 (a) C.F. Matta, J. Hernández-Trujillo, T.-H. Tang, and R.F.W. Bader, *Chem. Eur. J.*, 2003, **9**, 1940-1951; (b) J. Echeverría, G. Aullón, D. Danóvich, S. Shaik, and S. Alvarez, *Nat. Chem.*, 2011, **3**, 323-330.

22 (a) D.J. Wolstenholme and T.S. Cameron, *J. Phys. Chem. A*, 2006, **110**, 8970-8978; (b) E.A. Zhurova, C.F. Matta, N. Wu, V.V. Zhurov, and A.A. Pinkerton, *J. Am. Chem. Soc.*, 2006 **128**, 8849-8861.

23 (a) C.F. Matta, *In Hydrogen Bonding-New Insight*, (Challenges and advances in Computational Chemistry and Physics Series); S. Grabowski, Ed.; Springer, New York, 2006; (b) D.J. Wolstenholme, C.F. Matta, T.S. Cameron, *J. Phys. Chem. A*, 2007, **111**, 8803-8813.

24 R. Eisenschitz and F. London, *Z. Phys.*, 1930, **60**, 491-527.

25 R.F.W. Bader, *Atoms in Molecules: A Quantum Theory*, Oxford University Press, Oxford, U.K., 1990.

26 (a) T.S. Koritsanszky and P. Coppens, *Chem. Rev.*, 2001, **101**, 1583-1627; (b) F. Cortés-Guzmán, R.F.W. Bader, *Coord. Chem. Rev.*, 2005, **249**, 633-662; (c) W. Nakanishi, S. Hayashi, *Curr. Org. Chem.*, 2010, **14**, 181-197.

27 E. Espinosa, E. Molins, and C. Lecomte, *Chem. Phys. Lett.*, 1998, **285**, 170-173.

28 D.J. Wolstenholme and T.S. Cameron, *Can. J. Chem.*, 2007, **85**, 576-585.

29 (a) S.I. Orimo, Y. Nakamori, J.R. Eliseo, A. Züttel, and C.M. Jensen, *Chem. Rev.*, 2007, **107**, 4111-4132; (b) J. Graetz, *Chem. Soc. Rev.*, 2009, **38**, 73-82.



 

30 L. George and S.K. Saxena, *Int. J. Hydrogen Energ.*, 2010, **35**, 5454-5470.

31 P.F. Lang and B.C. Smith, *Dalton Trans.*, 2010, **39**, 7786-7791.

32 P. Sirsch, F.N. Che, J.T. Titah, and G.S. McGrady, *Chem. Eur. J.*, 2012, **18**, 9476-9480.

33 D.J. Wolstenholme, M.M.D. Roy, M.E. Thomas, and G.S. McGrady, *Chem. Commun.*, 2014, **50**, 3820-3823.

34 W. Grochala and P.P. Edwards, *Chem. Rev.*, 2004, **104**, 1283-1315.

35 P. Vajeeston, P. Ravindran, B.C. Hauback, H. Fjellvag, A. Kjekshus, S. Furuseth, and M. Hanfland, *Phys. Rev. B*, 2006, **73**, 224102.

36 T. Noritake, M. Aoki, S. Towata, Y. Seno, Y. Hirose, E. Nishibori, M. Takata, and M. Sakata, *Appl. Phys. Lett.*, 2002, **81**, 2008-2010.

37 S. Harder, J. Spielmann, J. Intemann, and H. Bandmann, *Angew. Chem. Int. Ed.*, 2011, **50**, 4156-4160.

38 J. Intemann, J. Spielmann, P. Sirsch, and S. Harder, *Chem. Eur. J.*, 2013, **19**, 8478-8489.

39 J. Intemann, P. Sirsch, and S. Harder, *Chem. Eur. J.*, 2014, **20**, 11204-11213.

40 R.W.P. Wagemans, J.H. van Lenthe, P.E. de Jongh, A.J. van Dillen, and K.P. de Jong, *J. Am. Chem. Soc.*, 2005, **127**, 16675-16680.

41 E.D. Jemmis, M.M. Balakrishnarajan, P.D. Pancharatna *J. Am. Chem. Soc.* **2001**, 123, 4313-4323.

42 H.W. Smith and W.N. Lipscomb *J. Chem. Phys.* **1965**, 43, 1060-1064.

43 L. Klebanoff, *Hydrogen Storage Technology, Materials, and Applications*, CRC Press, Taylor & Francis Group, Boca Raton, Fl., U.S.A., 2012.

44 J.W. Turley and H.W. Rinn, *Inorg. Chem.*, 1969, **8**, 18-22.

45 B.G. de Oliveira, *Phys. Chem. Chem. Phys.*, 2013, **15**, 37-79.

46 H.W. Brinks, A. Istad-Lem, and B.C. Hauback, *J. Phys. Chem. B*, 2006, **110**, 25833-25837.

47 F.N. Che, *Charge Density Studies of Lightweight Metal Hydrides for Hydrogen Storage*, PhD Thesis, University of New Brunswick, Fredericton, New Brunswick, Canada, 2012.

48 H.W. Brinks, W. Langley, C.M. Jensen, J. Graetz, J.J. Reilly, and B.C. Hauback, *J. Alloys Compd.*, 2007, **433**, 180-183.

49 (a) V.A. Yartys, R.V. Denys, J.P. Maehlen, Ch. Frommen, M. Fichtner, B.M. Bulychev, and H. Emerich, *Inorg. Chem.*, 2007, **46**, 1051-1055; (b) H.W. Brinks, C. Brown, C.M. Jensen, J. Graetz, J.J. Reilly, and B.C. Hauback, *J. Alloys Compd.*, 2007, **441**, 364-367.

50 L. Li, C. Xu, C. Chen, Y. Wang, L. Jiao, and H. Yuan, *Int. J. Hydrogen Energ.*, 2013, **38**, 8798-8812.

51 J.W. Lauher, D. Dougherty, P.J. Herley, *Acta Cryst.*, 1979, **B35**, 1454-1456.

52 E. Rönnebro, D. Noréus, K. Kadir, A. Reiser, and B. Bogdanović, *J. Alloys Compd.*, 2000, **299**, 101-106.

53 D.S. Marynick and W.N. Lipscomb, *Inorg. Chem.*, 1972, **11**, 820-823.

54 (a) A.R. Gerson and S.C. Nyburg, *Acta Cryst.*, 1994, **B54**, 252-256; (b) R. Boese, H.-C. Weiss, and D. Bläser, *Angew. Chem. Int. Ed.*, 1999, **38**, 988-992.

55 R.W. Broach, I. Chuang, T.J. Marks, and J.M. Williams, *Inorg. Chem.*, 1983, **22**, 1081-1084.

56 S. Aldridge, A.J. Blake, A.J. Downs, R.O. Gould, S. Parsons, and C.R. Pulham, *J. Chem. Soc., Dalton Trans.*, 1997, 1007-1012.

57 R.A. DiStasio Jr., V.V. Gobre, and A. Tkatchenko, *J. Phys.: Condens. Matter*, 2014, **26**, 213202.

58 (a) A. Staubitz, A.P.M. Robertson, and I. Manners, *Chem. Rev.*, 2010, **110**, 4079-4124; (b) Z. Huang and T. Autrey, *Energy Environ. Sci.*, 2012, **5**, 9257-9268.

59 (a) A. Staubitz, A.P.M. Robertson, M.E. Sloan, and I. Manners, *Chem. Rev.*, 2010, **110**, 4023-4078; (b) M. Bowden and T. Autrey, *Curr. Opin. Solid State Mater. Sci.*, 2011, **15**, 73-79.

60 C.W. Hamilton, R.T. Baker, A. Staubitz, and I. Manners, *Chem. Soc. Rev.*, 2009, **38**, 279-293.

61 A.C. Stowe, W.J. Shaw, J.C. Linehan, B. Schmid, and T. Autrey, *Phys. Chem. Chem. Phys.*, 2007, **9**, 1831-1836.

62 W.T. Klooster, T.F. Koetzler, P.E.M. Siegbahn, T.B. Richardson, R.H. Crabtree, *J. Am. Chem. Soc.*, 1999, **121**, 6337-6343.

63 (a) E.W. Hughes, *J. Am. Chem. Soc.*, 1956, **78**, 502-503; (b) E.L. Lippert and W.N. Lipscomb, *J. Am. Chem. Soc.*, 1956, **78**, 503-504.

64 N.J. Hess, G.K. Schenter, M.R. Hartman, L.L. Daemen, T. Proffen, S.M. Kathmann, C.J. Mundy, M. Hart, D.J. Heldebrant, A.C. Stowe, and T. Autrey, *J. Phys. Chem.*, 2009, **113**, 5723-5735.

65 M. Bowden, D.J. Heldebrant, A. Karkamkar, T. Proffen, G.K. Schenter, and T. Autrey, *Chem. Commun.*, 2010, **46**, 8564-8566.

66 D.J. Wolstenholme, K.T. Traboulsee, Y. Hua, L.A. Calhoun, and G.S. McGrady, *Chem. Commun.*, 2012, **48**, 2597-2599.

67 Monitoring the Raman spectra of freshly prepared samples of both $NH_3BD_3$ and $ND_3BH_3$ upon heating to 120 °C showed no signs for hydrogen scrambling in the decomposition of these isotopomers. D.J. Wolstenholme and G.S. McGrady, unpublished results

68 (a) Q.S. Li, J. Zhang, and S. Zhang, *Chem. Phys. Lett.*, 2005, **404**, 100-106; (b) J. Zhang, S. Zhang, and Q.S. Li, *Theochem*, 2005, **717**, 33-39.

69 M.T. Nguyen, V.S. Nguyen, M.H. Matus, G. Gopakumar, and D.A. Dixon, *J. Phys. Chem. A*, 2007, **111**, 679-690.

70 X. Chen, X. Bao, J.-C. Zhao, and S.G. Shore, *J. Am. Chem. Soc.*, 2011, **133**, 14172-14175.

71 (a) Z. Xiong, C.K. Yong, G. Wu, P. Chen, W. Shaw, A. Karkamkar, T. Autrey, M.O. Jones, S.R. Johnson, P.P. Edwards, and W.I.F. David, *Nat. Mater.*, 2008, **7**, 138-141; (b) Z. Xiong, G. Wu, Y.S. Chua, J. Hu, T. He, W. Xu, P. Chen, *Energy Environ. Sci.*, 2008, **1**, 360-363; (c) H. Wu, W. Zhou, and T. Yildirim, *J. Am. Chem. Soc.*, 2008, **130**, 14834-14839.

72 D.J. Wolstenholme, J.T. Titah, F.N. Che, K.T. Traboulsee, J. Flogeras, and G.S. McGrady, *J. Am. Chem. Soc.*, 2011, **133**, 16598-16604.

73 Y.S. Chua, P. Chen, G. Wu, and Z. Xiong, *Chem. Commun.*, 2011, **47**, 5116-5129.

74 T.B. Lee and M.L. McKee, *Inorg. Chem.*, 2009, **48**, 7564-7575.

75 D.Y. Kim, N.J. Singh, H.M. Lee, and K.S. Kim, *Chem Eur. J.*, 2009, **15**, 5598-5604.

76 A.T. Luedtke and T. Autrey, *Inorg. Chem.*, 2009, **48**, 3905-3910.

77 D.J. Wolstenholme, J. Flogeras, F.N. Che, A. Decken, and G.S. McGrady, *J. Am. Chem. Soc.*, 2013, **135**, 2439-2442.

78 D. Seyferth, D.Y. Son, A.L. Rheingold, and R.L. Ostrander *Organometallics*, 1994, **13**, 2682-2690.

79 S. Aldridge and A.J. Downs *Chem. Rev.*, 2001, **101**, 3305-3365.